In Vitro Cellular & Developmental Biology - Animal (2024) 60:333–342
https://doi.org/10.1007/s11626-024-00886-3

CDC-like kinase 3 deficiency aggravates hypoxia-induced cardiomyocyte apoptosis through AKT signaling pathway

Xiue Ma[1] · Liming Gao[2] · Rucun Ge[3] · Tianyou Yuan[4] · Bowen Lin[1] · Lixiao Zhen[3]

Received: 16 October 2023 / Accepted: 13 February 2024 / Published online: 4 March 2024 / Editor: John W. Harbell

Abstract
Hypoxia-induced cardiomyocyte apoptosis is one major pathological change of acute myocardial infarction (AMI), but the underlying mechanism remains unexplored. CDC-like kinase 3 (CLK3) plays crucial roles in cell proliferation, migration and invasion, and nucleotide metabolism, however, the role of CLK3 in AMI, especially hypoxia-induced apoptosis, is largely unknown. The expression of CLK3 was elevated in mouse myocardial infarction (MI) models and neonatal rat ventricular myocytes (NRVMs) under hypoxia. Furthermore, CLK3 knockdown significantly promoted apoptosis and inhibited NRVM survival, while CLK3 overexpression promoted NRVM survival and inhibited apoptosis under hypoxic conditions. Mechanistically, CLK3 regulated the phosphorylation status of AKT, a key player in the regulation of apoptosis. Furthermore, overexpression of AKT rescued hypoxia-induced apoptosis in NRVMs caused by CLK3 deficiency. Taken together, CLK3 deficiency promotes hypoxia-induced cardiomyocyte apoptosis through AKT signaling pathway.

Keywords CDC-like kinase 3 · Hypoxia · Cardiomyocyte apoptosis · AKT

Introduction

Acute myocardial infarction (AMI) is a critical illness in the clinic with high mortality and morbidity (Damluji *et al*. 2021; Gong *et al*. 2021; Zhang *et al*. 2022a, b). The wide application of vascular recanalization methods, such as intravenous coronary thrombolysis and percutaneous coronary intervention (Borer *et al*. 2002; Jellis *et al*. 2010; Mackman *et al*. 2020; Sabatine and Braunwald 2021; Schäfer *et al*. 2022), help save a lot of lives for AMI patients. Despite advancements in vascular recanalization methods, the irreversible damage caused by AMI continues to demand a deeper understanding of its underlying mechanisms.

During myocardial ischemia, the myocardium becomes profoundly hypoxic (Ruan *et al*. 2022; Fan *et al*. 2023). As a common consequence of AMI, hypoxia leads to severe cellular stress and even cell apoptosis (Yu *et al*. 2019; Pan *et al*. 2021). The AKT pathway is an important signaling pathway related to cardiomyocyte function. Activated AKT can promote the expression of antiapoptotic proteins, thereby preventing cell apoptosis (Wei *et al*. 2020; Wen *et al*. 2020; Cheng *et al*. 2021; Zhang *et al*. 2022a, b). Hypoxia-inducible factors (HIFs), especially HIF-1α, are activated in response to ischemia (Knutson *et al*. 2021; Hu *et al*. 2022). Moreover, $CoCl_2$ is known to mimic hypoxia-like conditions, making it a valuable tool in studying the cellular response to hypoxia (Hu *et al*. 2021; Liu *et al*. 2022).

The CDC-like kinase family, particularly CLK3, has emerged as a potential key player in myocardial ischemia. Unlike other CLK family members, the C-lobe of CLK3 contains conserved regions: the LAMMER motif, mitogen-activated insertion, the MAPK-like insertion; these different regions confer CLK3 with different affinities for various small-molecule compounds (Martín Moyano *et al*. 2020) and

✉ Tianyou Yuan
tianyou_yuan@163.com

✉ Bowen Lin
bowenlin0512@163.com

✉ Lixiao Zhen
zlxiao56@163.com

[1] School of Medicine, Tongji University, Shanghai 200092, China

[2] Department of Cardiology, Ji'an Hospital, Shanghai East Hospital, Ji'an 343000, Jiangxi, China

[3] Shandong Provincial Third Hospital, Shandong University, Jinan 250012, Shandong, China

[4] Department of Cardiology, Shanghai General Hospital, Shanghai Jiao Tong University School of Medicine, Shanghai 201620, China

impart distinct functional roles in cell proliferation, migration and invasion and nucleotide metabolism (Zhou *et al*. 2020). Moreover, CLK1 and CLK3 were reported as AKT target substrates, which may play a specific role in B cell signaling (Mohammad *et al*. 2016). Akt was also found to phosphorylate CLK2 at Serine 34 and Threonine 127 directly (Nam *et al*. 2010). Understanding the interplay between CLK3 and these hypoxia-responsive pathways could provide insights into novel therapeutic strategies for AMI treatment.

This study provides evidence that CLK3 was upregulated in myocardial infarction (MI) model mice and cobalt chloride ($CoCl_2$)-treated hypoxic neonatal rat ventricular myocytes (NRVMs). Notably, knockdown of CLK3 was found to exacerbate apoptosis induced by $CoCl_2$, while overexpression of CLK3 was shown to suppress hypoxia-induced apoptosis in NRVMs. Mechanistic exploration showed that the CLK3-AKT interaction regulates hypoxia-induced apoptosis. Importantly, our study shows that CLK3 was involved in MI pathogenesis.

Materials and methods

Animals Animal experiments were carried out in accordance with the National Institutes of Health Guidelines for the Use of Laboratory Animals, and all procedures were approved by the Animal Care Committee of Shandong Provincial Third Hospital (Shandong, China). The animals were housed in normal cages at a temperature of 24 ± 2°C and relative humidity of 60% on a 12:12 h light and dark cycle and given free access to water. To model MI, 8 ~ 10-week-old male C57BL/6 mice were subjected to MI surgery. The mice were randomly assigned to the sham and MI groups. Cardiomyocytes were isolated from neonatal Sprague–Dawley rats (1 ~ 3 d old).

Myocardial infarction surgery Eight-week-old male C57BL/6 mice in the MI group were anesthetized via 2% isoflurane inhalation and fixed on a heating pad in the left supine position. Left thoracotomy was performed at the 4th left intercostal space. The heart was subsequently exposed, and the pericardium was opened. The left anterior descending (LAD) artery was ligated with a 7–0 suture immediately below the tip of the left auricle. When the left ventricle became pale, LAD ligation was considered successful. The sham mice underwent the same procedure except occlusion of the LAD. Ensuring a hermetic closure of the surgical site, air was evacuated, and the chest was closed with 6–0 sutures. The mice were placed on another heating pad until recovery. At different time points after the operation, the hearts were analyzed.

Cardiomyocyte isolation, culture and treatments NRVMs were isolated from Sprague–Dawley rats (1 ~ 3 d old) using a differential adhesion method as described previously (Chen *et al*. 2019). Briefly, the heart was minced into 1 mm^3 fragments and digested with 0.1% collagenase type II (Worthington, LS004177, Lakewood, NJ) and 1% BSA in PBS. The cells were then separated into cardiomyocytes and cardiac fibroblasts via differential adhesion. NRVMs were used for subsequent experiments. The cells were cultured in high-glucose Dulbecco's Modified Eagle Medium (DMEM, GIBCO, c11995500bt , Waltham, MA) containing 20% M199 medium (Basal Media, L649KJ, Shanghai, China), 10% fetal bovine serum (FBS, EXCELL, FND500, Taicang, China), 100 μM 5-bromo-2'-deoxyuridine (Brdu, Sigma, B5002-250MG, St. Louis, MO) and 1 × penicillin–streptomycin (P/S, Gibco, 15,070,063, Waltham, MA). Afterward, the cells were cultured in high-glucose DMEM containing 20% M199 medium and 2% FBS.

Transfection was performed with Lipofectamine™ RNAimax transfection reagent (Invitrogen, 13,778,150, Carlsbad, CA) and Lipofectamine® 3000 transfection reagent (Invitrogen, L3000015, Carlsbad, CA) according to the manufacturer's instructions. Briefly, for the knockdown assay, small interfering RNA (siRNA) against *Clk3* (40 nmol/L) and negative control siRNA were transfected into NRVMs using Lipofectamine™ RNAimax transfection reagent. For the overexpression assay, 4 μg Flag-CLK3 plasmid (Sino Biological, HG10716-CF, Beijing, China), 4 μg Flag-vector plasmid (Sino Biological, CV012, Beijing, China), and 5 μL P3000 were mixed with 125 μL of Opti-MEM medium (GIBCO, 11,058–021, Waltham, MA). Then, 5 μL Lipofectamine™ 3000 was diluted in 125 μL Opti-MEM. After incubation for 5 min at RT, diluted DNA and diluted Lipofectamine™ 3000 were combined and incubated for another 15 min at RT. Afterward, DNA-lipid complex was added to each well. Forty-eight hours post-transfection, the medium was replaced with fresh complete medium containing 2% FBS and $CoCl_2$ or PBS for another 24 h. Finally, the NRVMs were collected for analysis. The siRNA sequences are listed in Table 1.

Table 1. The specific siRNA sequences

siRNA	Sense (5'-3')	Antisense (5'-3')
NC	UUCUCCGAACGUGUCACGUTT	ACGUGACACGUUCGGAGAATT
Rat-*Clk3* #1	GGUCGACUACGAUACCCAUTT	GGUCGACUACGAUACCCAUTT
Rat-*Clk3* #2	GGAGUGUGGAAGAUGACAATT	UUGUCAUCUUCCACACUCCTT
Rat-*Clk3* #3	GGAAGCUGCUCGUCUAGAATT	UUCUAGACGAGCAGCUUCCTT

Cell culture Human embryonic kidney 293 T (HEK293T) cells were obtained from Shanghai Zhong Qiao Xin Zhou Biotechnology (ZQ0033, Shanghai, China). The cell line used in this study was tested and authenticated. We confirmed that all experiments used mycoplasma-free cells. HEK293T cells were cultured in DMEM supplemented with 10% FBS and 1% penicillin streptomycin (P/S), and incubated at 37°C with 5% CO_2.

Quantitative real-time polymerase chain reaction (qRT-PCR) Total RNA was extracted from NRVMs and heart tissues using RNAiso Plus (Takara, 9109, Shiga, Japan) according to the manufacturer's instructions. The concentration and purity of the RNA samples were determined using a Nanodrop 2000 spectrophotometer (Thermo Fisher Scientific). cDNA was synthesized using PrimeScript™ RT Master Mix (Takara, RR036A, Shiga, Japan). Real-time PCR was conducted using SYBR Green Real-Time PCR Master Mix (TOYOBO, QPK-201, Osaka, Japan). β-Actin was used as an internal reference. The sequences of the primers used for PCR in this study are listed in Table 2.

Western blotting analysis Total protein was extracted from cells or tissues by RIPA lysis buffer (Beyotime, P0013B, Shanghai, China) containing protease inhibitor (Roche, 4,906,845,001, 1 ml ddH_2O per tablet, 1:50, Mannheim, Germany) and phosphatase inhibitor (Roche, 4,693,116,001, 400 µL ddH2O per tablet, 1:25, Mannheim, Germany) on ice for 30 min. Subsequently, the lysates were centrifuged at 12,000 × g and 4°C for 15 min. The concentration of the protein was measured using a BCA kit (Beyotime, P0009). The protein lysates (35 µg protein per sample) were separated on a 10% NuPAGE Bis–tris gel (Invitrogen, NP0316BOX, Carlsbad, CA) and transferred to PVDF membranes (Millipore, IPVH00010, Burlington, MA). The membranes were then blocked with 5% nonfat milk at RT for 1 h and subsequently incubated with primary antibodies (β-Actin, 1:1000, Santa Cruz, sc-47778, Dallas, TX; CLK3, 1:200, Cell Signaling Technology, 3256, Danvers, MA; HIF-1α, 1:1000, Cell Signaling Technology, 36,169; PARP, 1:1000, Cell Signaling Technology, 9532; Bcl-2, 1:500, Santa Cruz, sc-7382; Bax, 1:1000, Cell Signaling Technology, 2772; Caspase-3, 1:200, Cell Signaling Technology, 9662; Akt, 1:1000, Abcam, ab8805, Cambridge, UK; Phospho-Akt (Ser473), 1:1000, Cell Signaling Technology, 4060 T; Anti-Phospho-(Ser/Thr), 1:500, Abcam, ab300625; p53 (DO-1), 1:200, Santa Cruz, sc-126; p53 (DO-2), 1:200, Santa Cruz, sc-53394) at 4°C overnight. The next day, TBS containing 0.1% Tween 20 (TBST) was used to rinse the membranes. Subsequently, the membranes were incubated with near infrared dyes-conjugated secondary antibodies (Invitrogen, A32735; Invitrogen, A21036, Carlsbad, CA) at RT for 1 h. Images of the protein bands were captured using an Odyssey imager (LI-COR, Biosciences). Then, the band intensity was quantified using ImageJ software (version 1.46r). β-Actin was used as a loading control.

Immunofluorescence and TUNEL staining NRVMs were fixed in 4% paraformaldehyde for 15 min and permeabilized with 0.5% Triton X-100 in PBS for 15 min. After washing, the cells were blocked with 5% normal goat serum at RT for 1 h. The cells were then incubated with primary antibody against cardiac troponin T (cTnT, 1:500, Abcam, ab8295, Cambridge, UK) at RT for 1 h or overnight at 4°C. The cells were washed three times with PBS with 0.1% Tween 20 (PBST) and incubated for 1 h with Alexa Fluor® 488-conjugated goat anti-mouse IgG secondary antibody (1:500, Abcam, ab150113, Cambridge, UK). Apoptotic cells were stained using reagents from an In Situ Cell Death Detection Kit, TMR Red (Roche, 12,156,792,910, Mannheim, Germany) for 1 h. The cells were washed three times with PBS, and nuclei were stained with DAPI (1:1000, Sigma, D9542, St. Louis, MO) for 15 min. Images were captured using a fluorescence microscope (Leica, DMi8). At least 6 random images from each group were analyzed.

Cell counting kit-8 (CCK-8) assay Cell viability was measured using the CCK-8 assay according to the manufacturer's protocol (Beyotime, C0038, Shanghai, China). Briefly, NRVMs were seeded in 96-well plates and cultured in high-glucose DMEM containing 20% M199 medium and 2% FBS in a humidified 5% CO_2 incubator at 37°C. Forty-eight hours post-transfection, the cells were treated with $CoCl_2$ at a final concentration of 400 µM. Ten microliters of CCK-8 solution mixed with 100 µL of medium was added to each well after 24 h of treatment with $CoCl_2$, and the cells were incubated for another 4 h. The absorbance of each well was measured at 450 nm using an M5 Molecular Devices microplate reader.

Table 2. The primer sequences

Genes	Primer sequences (Forward)	Primer sequences (Reverse)
Mouse-*Clk3* #1	GTATCGGTGTGAAGAGCGGA	GCTTACTGCTCTGTTGGCTTC
Mouse-*Clk3* #2	GTGTGGAAGATGACAAGGAGGG	ATCTTCAGGGCAACCTGTGAC
Mouse-*Gapdh*	TGAAGGTCGGTGTGAACGGATTTGG	ACGACATACTCAGCACCAGCATCAC
Rat-*Clk3* #1	TCCGTAATGTGGGCAAGTACC	ACCAGTCAGACATCAGGACAC
Rat-*Clk3* #2	CATCACACCACCATTGTCGC	TTCTGCTTCCTGGTACGGTG
Rat-*β-actin*	CCCATCTATGAGGGTTACGC	TTTAATGTCACGCACGATTTC

Immunoprecipitation (IP) HEK293T cells were transfected with either AKT plasmid alone or co-transfected with Flag and CLK3-Flag plasmids. 48 h post-transfection, the cells were washed three times with pre-cooled PBS and then lysed with 800 µL lysis buffer (RIPA buffer with protease inhibitor and phosphatase inhibitor). The samples were incubated on ice for 30 min and then centrifuged at 12,000 g at 4°C for 15 min. 30–50 µL of the extracted protein was kept as the input sample. Concurrently, magnetic beads (Thermo Fisher Scientific, 88,803, Waltham, MA) were gently mixed, and 30 µL per sample was used and mixed on a rotator. Beads were allowed to settle on a magnetic rack for over 30 s before supernatant removal. After washing, 500 µL of PBST-mixed beads were added to each tube, and the appropriate volume of Flag antibody (1:500, Sigma, F1804-200UG, St. Louis, MO) was added. The mixture was incubated at room temperature on a rotator for 1.5 to 2 h. The beads, now bound to the antibody, were gently washed with PBS and mixed on a rotator three times. After magnetic separation and supernatant removal, the rest of the protein was added to the bead tubes and incubated at 4°C overnight on a rotator. The following day, samples were washed three times with PBS, boiled at 100°C for 10 min in the loading buffer and used for subsequent experiments.

Statistical analysis The data are presented as the mean ± SEM, and all data were at least three different experiments. A P value < 0.05 was considered significant difference. Statistical analyses were carried out using GraphPad Prism software (version 6.01). Two-tailed Student t-test, and one-way analysis of variance (ANOVA) and two-way ANOVA were carried out as appropriate.

Results

The expression of CLK3 is upregulated in myocardial infarction tissues and NRVMs exposed to hypoxia To investigate the function of CLK3 in cardiomyocyte apoptosis, we first measured the expression of CLK3 in adult mice (C57BL/6) after MI injury. The mRNA expression of *Clk3* was increased on 1 d, 3 d and 5 d post-MI (Fig. 1*A* and Supplementary Fig. S1*A*). We subsequently measured the expression of CLK3 in NRVMs exposed to varying concentrations of $CoCl_2$ (200, 300, 400, and 600 µM). Similar to what was observed in mice, the expression of CLK3 was significantly upregulated in a dose-dependent manner in NRVMs following $CoCl_2$-induced hypoxic injury (Fig. 1*B*, *C*). The mRNA expression of *Clk3* also yielded similar outcomes (Supplementary Fig. S1***B***, ***C***). These findings demonstrated that CLK3 might have a potential role in hypoxia-induced apoptosis in cardiomyocytes.

CLK3 deficiency aggravates hypoxia-induced NRVM apoptosis To verify the function of CLK3 in cardiomyocytes, we knocked down *Clk3* in NRVMs with an siRNA. We designed three siRNAs targeting various regions of *Clk3*, and the knockdown efficiency of the *Clk3* siRNAs was assessed by qRT-PCR. The mRNA expression of *Clk3* was significantly downregulated 72 h post-siRNA transfection, indicating that we successfully knocked down *Clk3*, and si-*Clk3* #3 had the highest knockdown efficiency (Fig. 2*A*, Supplementary Fig. S2). We first measured the expression of the HIF-1α protein to confirm that $CoCl_2$ caused hypoxic injury to the NRVMs (Fig. 2*B*). To assess the role of CLK3 in hypoxia-induced NRVM apoptosis, we evaluated the expression levels of apoptosis-related proteins, such as PARP, Bcl-2, Bax, and Caspase-3. We found that the cleaved to total PARP ratio, the cleaved to total Caspase-3 ratio, and the Bax/Bcl2 ratio were increased in NRVMs with CLK3 knockdown compared to control NRVMs (Fig. 2*B-E*). The TUNEL assay was carried out to determine the level of apoptosis. The TUNEL-positive cell number was further increased by CLK3 depletion under hypoxia (Fig. 2*F*, *G*). Moreover, depletion of CLK3 markedly reduced NRVM viability under hypoxia, as determined by the CCK- 8 assay (Fig. 2*H*). We also speculated on the role of CLK3 in regulating the

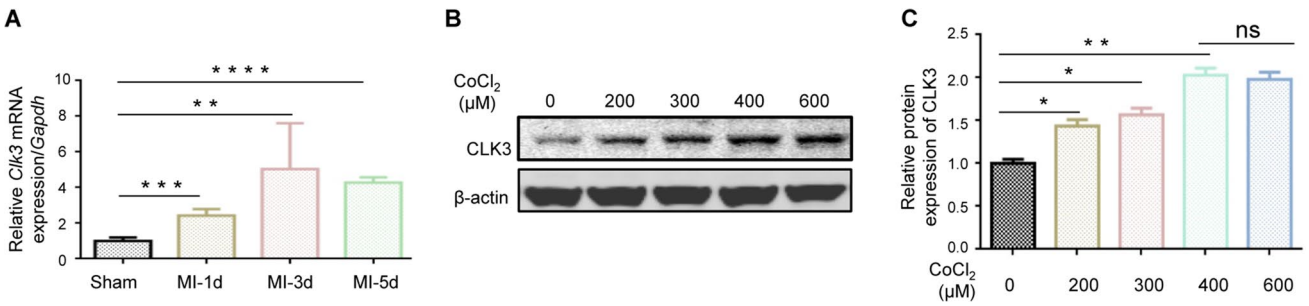

Figure 1. Expression of CLK3 was upregulated in cardiomyocytes under hypoxic conditions. (*A*) mRNA expression of *Clk3* in C57BL/6 mice heart on 1 d, 3 d and 5 d post-MI using mouse-Clk3 primer #1. GAPDH was utilized as an internal reference gene; n = 5 mice per group. (*B*, *C*) Protein expression of CLK3 in NRVMs exposed to different concentrations of $CoCl_2$ or PBS for 24 h. β-Actin served as a loading control, n = 3 independent experiments. Values represent the mean ± SEM. Statistical significance: $^*P < 0.05$, $^{**}P < 0.01$, $^{***}P < 0.001$, $^{****}P < 0.0001$, ns, not significant.

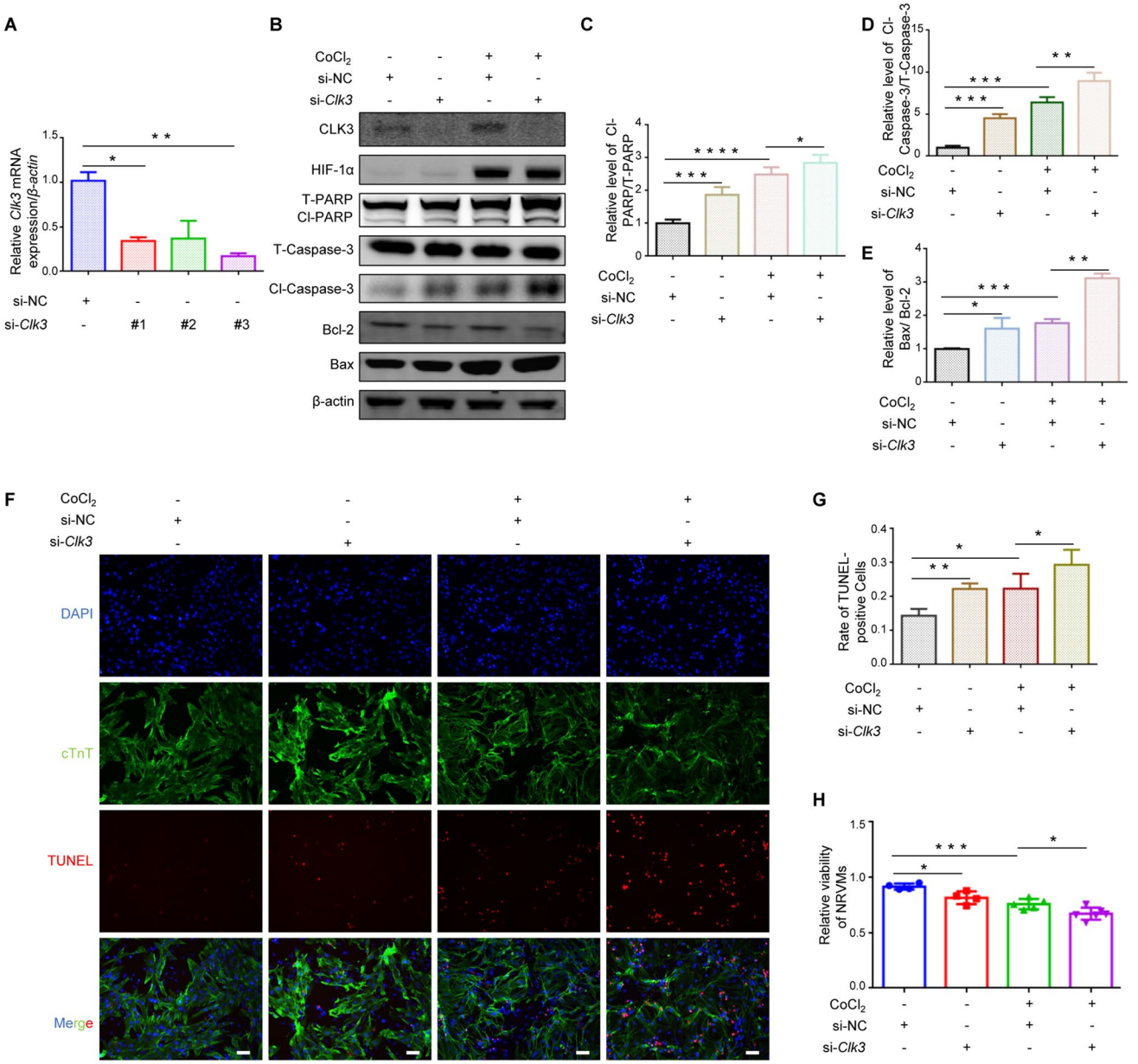

Figure 2. Silencing of *Clk3* aggravated hypoxia-induced NRVMs apoptosis. (*A*) qRT-PCR analysis of *Clk3* in NRVMs transfected with *Clk3* siRNA. n = 3 independent experiments. (*B-E*) Western Blot analysis of apoptosis-related proteins in NRVMs treated with or without $CoCl_2$ after *Clk3* siRNA transfection. n = 3 independent experiments. (*F-G*) TUNEL assay for cell apoptosis analysis in NRVMs treated with or without $CoCl_2$ after *Clk3* siRNA transfection. n = 3 independent experiments. Scale bar: 50 μm. (*H*) CCK-8 assay for cell viability analysis in NRVMs treated with or without $CoCl_2$ after *Clk3* siRNA transfection. n = 3 independent experiments. Values represent the mean ± SEM. Statistical significance: $^{*}P < 0.05$, $^{**}P < 0.01$, $^{***}P < 0.001$, $^{****}P < 0.0001$.

splicing of apoptosis-related proteins P53. As indicated, CLK3 did not alter the splicing pattern of P53 proteins (Supplementary Fig. S3). These findings demonstrated that CLK3 deficiency critically contributes to NRVM apoptosis under hypoxic condition.

CLK3 overexpression inhibits apoptosis in NRVMs under hypoxia To further investigate the function of CLK3 exposed to $CoCl_2$-induced hypoxia, we overexpressed CLK3 using the CLK3 plasmid (Fig. 3*A*). We found that overexpression of CLK3 decreased the expression of apoptosis-related proteins in NRVMs, such as the ratios of cleaved to total PARP and Caspase-3, Bax/Bcl2 (Fig. 3*A-D*). Similarly, overexpression of CLK3 decreased the TUNEL-positive cell number (Fig. 3*E*, *F*). Moreover, the viability of NRVMs with CLK3 overexpression was higher than that of normal

NRVMs, as determined by the CCK-8 assay (Fig. 3*G*). These findings suggested that CLK3 could inhibit NRVM apoptosis under hypoxic condition.

CLK3 influences NRVM apoptosis via disrupting the AKT pathway Here, in CLK3 knockdown NRVMs, total AKT (t-AKT) levels remained consistent; however, there was a noticeable decrease in phosphorylated AKT (p-AKT) and p-AKT/t-AKT levels; this reduction became more severe in the presence of $CoCl_2$ treatment (Fig. 4*A-D*). Conversely, CLK3 overexpression resulted in an elevation of p-AKT levels and effectively rescued the downregulation

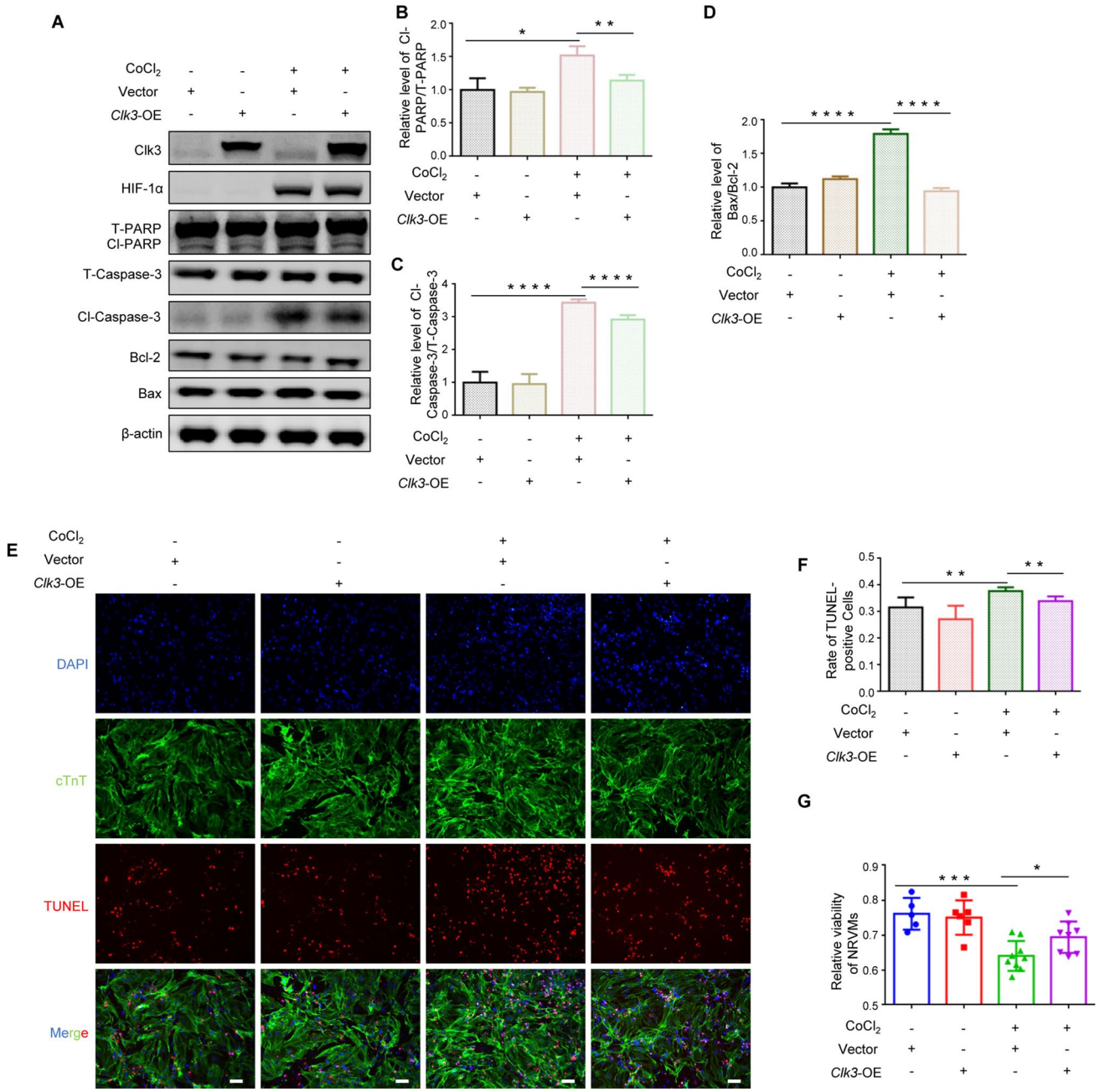

Figure 3. Overexpression of CLK3 inhibited $CoCl_2$-induced apoptosis in NRVMs. (*A-D*) Western Blot analysis of CLK3 and apoptosis-related proteins cell apoptosis in NRVMs treated with or without $CoCl_2$ after transfection with Flag-CLK3 or Flag-vector plasmid. n = 3 independent experiments. (*E*, *F*) TUNEL assay for cell apoptosis analysis in NRVMs treated with or without $CoCl_2$ after transfection with Flag-CLK3 or Flag-vector plasmid. n = 3 independent experiments. *Scale bar*: 50 μm. (*G*) CCK-8 assay for cell viability analysis in NRVMs treated with or without $CoCl_2$ after transfection with Flag-CLK3 or Flag-vector plasmid. n = 3 independent experiments. Values represent the mean ± SEM. Statistical significance: $^{*}P < 0.05$, $^{**}P < 0.01$, $^{***}P < 0.001$, $^{****}P < 0.0001$.

of p-AKT and p-AKT/t-AKT induced by $CoCl_2$ (Fig. 4*E-H*). As Akt was also reported to phosphorylate CLK2 (Nam *et al*. 2010), we wondered whether Akt might regulate the phosphorylation of CLK3. We performed immunoprecipitation experiments (using Flag antibody) in 293 T cells overexpressing Akt-OE and Flag-Vec or Flag-CLK3. Immunoblotting (IB) of the Phospho-Ser/Thr showed little difference between Flag-Vec or Flag-CLK3 (Supplementary Figure S4), reflecting that Akt might not phosphorylate CLK3. In summary, we found that CLK3 regulated the AKT phosphorylation in NRVM.

AKT rescues NRVM apoptosis caused by CLK3 deficiency under hypoxic condition To investigate whether the AKT pathway is involved in regulating NRVM apoptosis. We first overexpressed AKT using an AKT-expressing plasmid (Fig. 5*A*). Akt-OE did not affect the cleaved to total PARP and Bax/Bcl2 ratios but decreased cleaved to total Caspase-3 under $CoCl_2$-induced hypoxia (Supplementary Fig. S5). Importantly, we found that Akt-OE protected CLK3-deficient NRVMs from apoptosis, altered the expression of apoptotic proteins, and decreased the cleaved to total PARP, cleaved to total Caspase-3 and Bax/Bcl2 ratios under hypoxia (Fig. 5*B-E*). These results suggested that overexpression of AKT protected NRVMs against apoptosis induced by CLK3 deficiency under hypoxia.

Discussion

Currently, AMI stands as a prevalent and critical clinical condition (Damluji *et al*. 2021; Gong *et al*. 2021; Zhang *et al*. 2022a, b). AMI causes irreversible damage to myocardial and non-myocardial cells. The mortality rate of the disease remains high despite advances in revascularization therapies (Borer *et al*. 2002; Jellis *et al*. 2010; Sabatine and Braunwald 2021; Schäfer *et al*. 2022). New therapeutic strategies improving cardiac function after MI are urgently needed. CLK3 plays crucial roles in cellular processes, including cell proliferation, migration, and development (Cesana *et al*. 2018; Zhou *et al*. 2020; Virgirinia *et al*. 2021). In this study, we found that the expression of CLK3 was upregulated in mouse MI models and NRVMs exposed to $CoCl_2$ (a hypoxia mimetic). In further experiments, we found that CLK3 deficiency aggravated apoptosis and inhibited NRVM survival under hypoxic conditions. while CLK3 overexpression promoted NRVM survival and decreased apoptosis under hypoxia. These findings highlight the potential role of CLK3 in hypoxia-induced apoptosis in cardiomyocytes.

CLK3, a dual-specificity kinase, was reported to act as a protein kinase or a regulator of gene splicing in the past researches. As a protein kinase, CLK3 could directly phosphorylate USP13 at Y708 and influence the progression of cholangiocarcinoma (Zhou *et al*. 2020). The structure basis

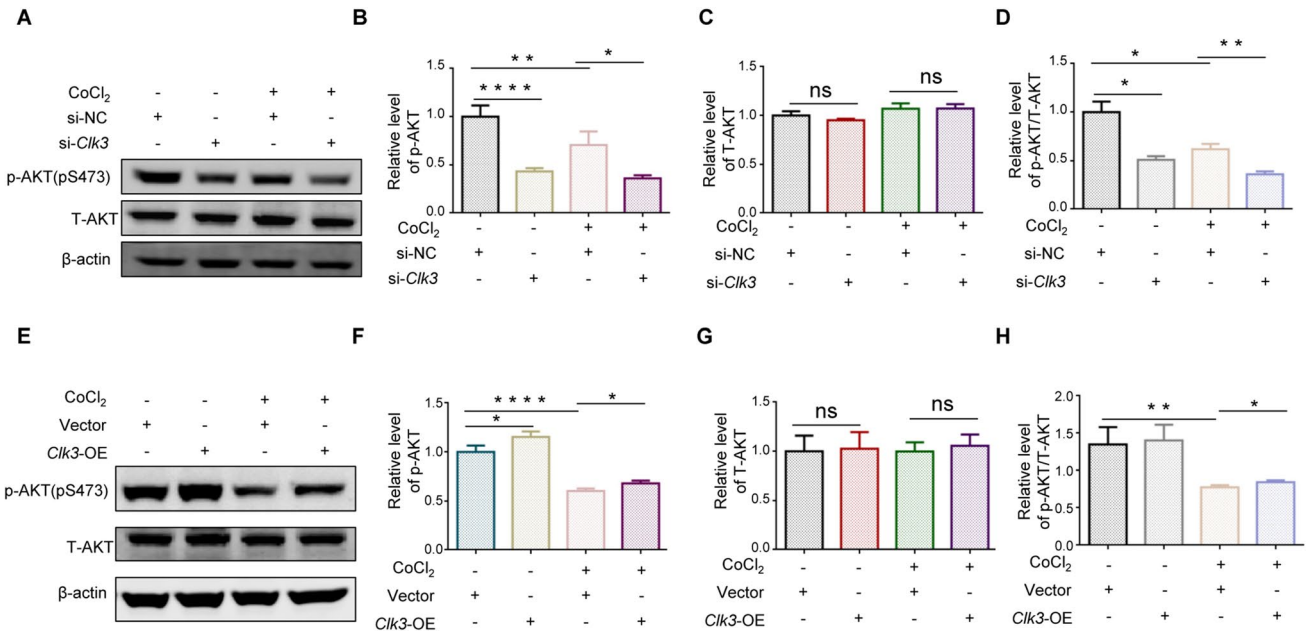

Figure 4. CLK3 influenced NRVMs apoptosis by disrupting the AKT pathway. (*A-D*) Western Blot analysis and quantification of p-AKT, t-AKT and p-AKT/t-AKT expression in CLK3-deficient NRVMs treated with or without $CoCl_2$. n = 3 independent experiments. (*E–H*) Western Blot analysis and quantification of p-AKT, t-AKT and p-AKT/t-AKT expression in CLK3-overexpressing NRVMs treated with or without $CoCl_2$. n = 3 independent experiments. Values represent the mean ± SEM. Statistical significance: $^*P < 0.05$, $^{**}P < 0.01$, $^{****}P < 0.0001$.

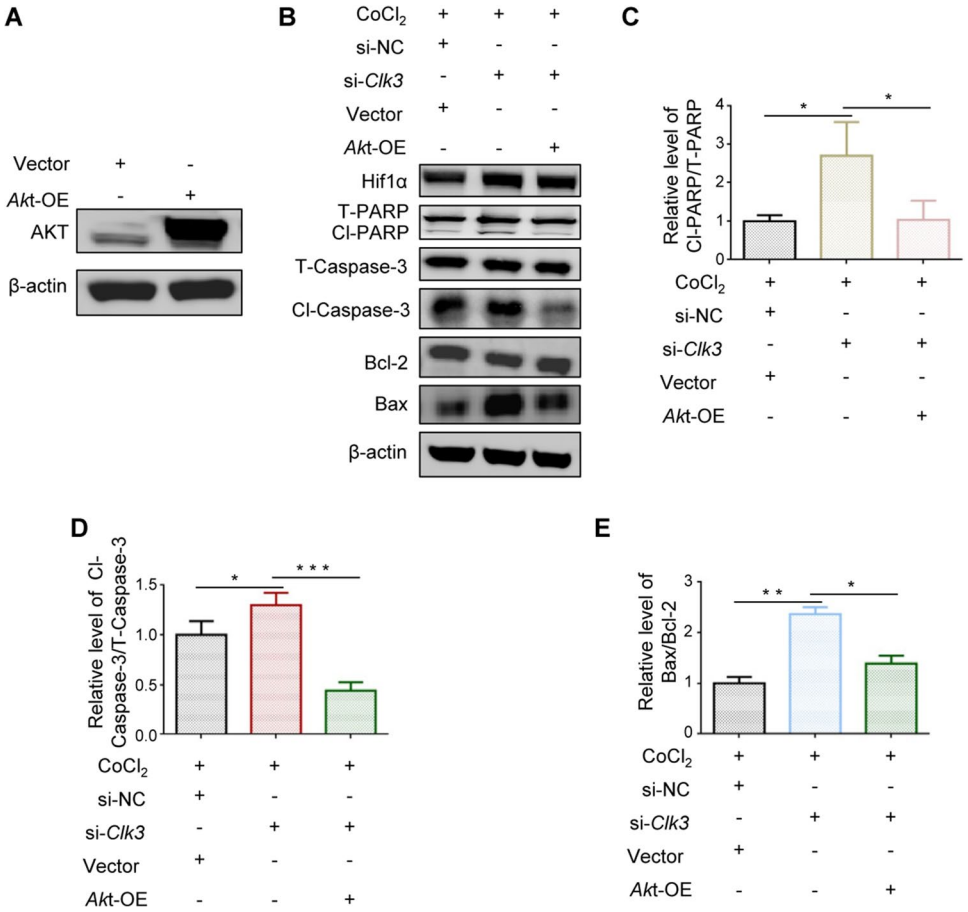

Figure 5. AKT rescued apoptosis in NRVMs caused by CLK3 deficiency under hypoxic condition. (*A*) The efficiency of AKT-overexpressing plasmid (*Akt*-OE) in NRVMs analyzed by Western Blot. n = 4 independent experiments. (*B*) Western Blot analysis of apoptosis in NRVMs treated with *Akt*-OE or not after exposure to hypoxia. n = 3 independent experiments. (*C-E*) Quantification of apoptosis-related proteins. n = 3 independent experiments. Values represent the mean ± SEM. Statistical significance: $^{*}P < 0.05$, $^{**}P < 0.01$, $^{***}P < 0.001$.

of CLK3's kinase function is that the catalytic domains of CLK3 present a typical protein kinase fold, with the C terminus displaying a unique and conserved conformation of EHLAMMERILG characteristic motif (Bullock *et al*. 2009). In this study, we found that CLK3 might regulate the phosphorylation of Akt (an important protein related to cardiomyocyte function) in NRVM. It remains to be figured out whether CLK3 also phosphorylate other proteins in cardiomyocytes and whether CLK3 phosphorylates Akt is a widespread phenomenon in other cells.

As a splicing regulator, CLK3 could regulate HMGA2 splicing, preserves HMGA2 function, and influences human hematopoietic stem cell (HSC) properties during development (Cesana *et al*. 2018). We also checked whether CLK3 regulates the splicing of p53 (an apoptosis-related protein). Although we did not observe p53 splicing pattern changes, we could not exclude the splicing regulator function of CLK3. Further genome-wide RNA sequencing might be needed to decipher how CLK3 regulates the RNA splicing.

Our research found that CLK3 deficiency contributed to NRVM apoptosis and disrupted the AKT pathway. AKT, a serine/threonine protein kinase, regulates cell apoptosis through influencing the expression levels of apoptosis-related proteins. Activated AKT can promote the expression of anti-apoptosis proteins, thereby preventing cell apoptosis. In recent years, AKT was shown to regulate the expression of apoptosis-related factors in cells (Wei *et al*. 2020; Wen *et al*. 2020; Li *et al*. 2021; Zhang *et al*. 2022a, b). The AKT pathway is an important signaling pathway related to cardiomyocyte function. Previous studies have found that Apocynum venetum leaf extract (AVLE) confers cardio-protection and alleviates doxorubicin-induced cardiotoxicity by suppressing oxidative stress and apoptosis of cardiomyocytes via the AKT/Bcl-2 signaling pathway (Zhang *et al*. 2022a, b). Mesenchymal stem cell (MSC)-derived exosomes ameliorate cardiomyocyte apoptosis under hypoxic conditions via the PTEN/AKT pathway (Sun *et al*. 2019; Wen *et al*. 2020). These findings demonstrate that the AKT pathway is an important signaling pathway related to cardiomyocyte apoptosis. In our study, we found that CLK3 influenced NRVM apoptosis and survival by disrupting the AKT pathway. CLK3 regulated the phosphorylation status of AKT. CLK3 deficiency led to reduced p-AKT expression while overexpression of CLK3 increased p-AKT levels. Furthermore, overexpression of AKT altered apoptotic protein expression and protected against apoptosis in NRVMs caused by CLK3 deficiency under hypoxia. In

result, CLK3 deficiency promotes hypoxia-induced cardiomyocyte apoptosis through AKT signaling pathway.

The findings above suggest that CLK3 is involved in cardiomyocyte apoptosis, possibly through its impact on the AKT signaling pathway. These results contribute to our understanding of the molecular mechanisms underlying cardiomyocyte survival and apoptosis regulation, offering insights into potential therapeutic strategies for myocardial infarction. However, whether CLK3 could regulate cardiomyocyte apoptosis in mouse MI models needs to be explored in further work. Further research is needed to elucidate the precise mechanisms by which CLK3 interacts with the AKT pathway and to explore its potential as a target for cardiac therapies.

Conclusions

Taken together, the CLK3-AKT interaction regulates hypoxia-induced cardiomyocyte apoptosis. These results contribute to our understanding of the molecular mechanisms underlying cardiomyocyte survival and apoptosis regulation, offering insights into potential therapeutic strategies for myocardial infarction.

Supplementary Information The online version contains supplementary material available at https://doi.org/10.1007/s11626-024-00886-3.

Author contributions Lixiao Zhen, Bowen Lin, and Tianyou Yuan conceived and designed experiments. Xiue Ma, Liming Gao and and Rucun Ge performed experiments, analyzed data, and prepared figures. Xiue Ma made the original draft preparation. Bowen Lin revised the manuscript. All authors have read and agreed to the published version of the manuscript.

Funding This research was funded by Medical and Health Science and Technology Development Program of Shandong Province (202103010947), the Scientific Research Foundation of Shandong Provincial Third Hospital (Q2023001), Key R&D Program of Shandong Province, China (2019GSF108249), and Jiangxi Province Municipal Health Commission Science Technology Grant (202210097).

Data availability The data that support the findings of this study are available from the corresponding author upon reasonable request.

Declarations

Conflicts of interest The authors declare no conflict of interest.

References

Borer JS, Truter S, Herrold EM, Falcone DJ, Pena M, Carter JN, Dumlao TF, Lee JA, Supino PG (2002) Myocardial fibrosis in chronic aortic regurgitation: molecular and cellular responses to volume overload. Circulation 105:1837–1842

Bullock AN, Das S, Debreczeni JE, Rellos P, Fedorov O, Niesen FH, Guo K, Papagrigoriou E, Amos AL, Cho S, Turk BE, Ghosh G, Knapp S (2009) Kinase domain insertions define distinct roles of CLK kinases in SR protein phosphorylation. Structure 17:352–362

Cesana M, Guo MH, Cacchiarelli D, Wahlster L, Barragan J, Doulatov S, Vo LT, Salvatori B, Trapnell C, Clement K, Cahan P, Tsanov KM, Sousa PM, Tazon-Vega B, Bolondi A, Giorgi FM, Califano A, Rinn JL, Meissner A, Hirschhorn JN, Daley GQ (2018) A CLK3-HMGA2 alternative splicing axis impacts human hematopoietic stem cell molecular identity throughout development. Cell Stem Cell 22:575-588.e577

Chen Y, Li X, Li B, Wang H, Li M, Huang S, Sun Y, Chen G, Si X, Huang C, Liao W, Liao Y, Bin J (2019) Long non-coding RNA ECRAR triggers post-natal myocardial regeneration by activating ERK1/2 signaling. Mol Ther 27:29–45

Cheng Y, Shen A, Wu X, Shen Z, Chen X, Li J, Liu L, Lin X, Wu M, Chen Y, Chu J, Peng J (2021) Qingda granule attenuates angiotensin II-induced cardiac hypertrophy and apoptosis and modulates the PI3K/AKT pathway. Biomed Pharmacother 133:111022

Damluji AA, van Diepen S, Katz JN, Menon V, Tamis-Holland JE, Bakitas M, Cohen MG, Balsam LB, Chikwe J (2021) Mechanical complications of acute myocardial infarction: a scientific statement from the american heart association. Circulation 144:e16–e35

Fan M, Yang K, Wang X, Chen L, Gill PS, Ha T, Liu L, Lewis NH, Williams DL, Li C (2023) Lactate promotes endothelial-to-mesenchymal transition via Snail1 lactylation after myocardial infarction. Sci Adv 9:eadc9465

Gong FF, Vaitenas I, Malaisrie SC, Maganti K (2021) Mechanical complications of acute myocardial infarction: a review. JAMA Cardiol 6:341–349

Hu X, Liu H, Li M, Zhu J, Yu Z (2021) Transcriptomic analysis reveals the role of a peptide derived from CRYAB on the CoCl(2)-induced hypoxic HL-1 cardiomyocytes. J Thromb Thrombolysis 51:265–276

Hu Y, Lu H, Li H, Ge J (2022) Molecular basis and clinical implications of HIFs in cardiovascular diseases. Trends Mol Med 28:916–938

Jellis C, Martin J, Narula J, Marwick TH (2010) Assessment of nonischemic myocardial fibrosis. J Am Coll Cardiol 56:89–97

Knutson AK, Williams AL, Boisvert WA, Shohet RV (2021) HIF in the heart: development, metabolism, ischemia, and atherosclerosis. J Clin Invest 131:e137557

Li J, Lin X, Chu J, Wu X, Chen X, Liu L, Shen A, Wu M, Peng J, Shen ZJB, Biomedecine p, pharmacotherapie (2021) Qingda granule attenuates angiotensin II-induced cardiac hypertrophy and apoptosis and modulates the PI3K/AKT pathway. Biomed Pharmacother 133:111022

Liu M, Liu P, Zheng B, Liu Y, Li L, Han X, Liu Y, Chu L (2022) Cardioprotective effects of alantolactone on isoproterenol-induced cardiac injury and cobalt chloride-induced cardiomyocyte injury. Int J Immunopathol Pharmacol 36:1–18

Mackman N, Bergmeier W, Stouffer GA, Weitz JI (2020) Therapeutic strategies for thrombosis: new targets and approaches. Nat Rev Drug Discov 19:333–352

Martín Moyano P, Němec V, Paruch K (2020) Cdc-Like Kinases (CLKs): biology, chemical probes, and therapeutic potential. Int J Mol Sci 21:7549

Mohammad DK, Ali RH, Turunen JJ, Nore BF, Smith CI (2016) B cell receptor activation predominantly regulates AKT-mTORC1/2 substrates functionally related to RNA processing. PLoS One 11:e0160255

Nam SY, Seo HH, Park HS, An S, Kim JY, Yang KH, Kim CS, Jeong M, Jin YW (2010) Phosphorylation of CLK2 at serine 34 and

threonine 127 by AKT controls cell survival after ionizing radiation. J Biol Chem 285:31157–31163
Pan F, Xu X, Zhan Z, Xu Q (2021) 6-Gingerol protects cardiomyocytes against hypoxia-induced injury by regulating the KCNQ1OT1/miR-340-5p/PI3K/AKT pathway. Panminerva Med 63:482–490
Ruan W, Ma X, Bang IH, Liang Y, Muehlschlegel JD, Tsai KL, Mills TW, Yuan X, Eltzschig HK (2022) The hypoxia-adenosine link during myocardial ischemia-reperfusion injury. Biomedicines 10:1939
Sabatine MS, Braunwald E (2021) Thrombolysis In Myocardial Infarction (TIMI) Study Group: JACC Focus Seminar 2/8. J Am Coll Cardiol 77:2822–2845
Schäfer A, König T, Bauersachs J, Akin M (2022) Novel therapeutic strategies to reduce reperfusion injury after acute myocardial infarction. Curr Probl Cardiol 47:101398
Sun XH, Wang X, Zhang Y, Hui J (2019) Exosomes of bone-marrow stromal cells inhibit cardiomyocyte apoptosis under ischemic and hypoxic conditions via miR-486-5p targeting the PTEN/PI3K/AKT signaling pathway. Thromb Res 177:23–32
Virgirinia RP, Nakamura M, Takebayashi-Suzuki K, Fatchiyah F, Suzuki A (2021) The dual-specificity protein kinase Clk3 is essential for Xenopus neural development. Biochem Biophys Res Commun 567:99–105
Wei L, Zhou Q, Tian H, Su Y, Fu GH, Sun T (2020) Integrin β3 promotes cardiomyocyte proliferation and attenuates hypoxia-induced apoptosis via regulating the PTEN/Akt/mTOR and ERK1/2 pathways. Int J Biol Sci 16:644–654
Wen Z, Mai Z, Zhu X, Wu T, Chen Y, Geng D, Wang J (2020) Mesenchymal stem cell-derived exosomes ameliorate cardiomyocyte apoptosis in hypoxic conditions through microRNA144 by targeting the PTEN/AKT pathway. Stem Cell Res Ther 11:36
Yu H, Chen B, Ren Q (2019) Baicalin relieves hypoxia-aroused H9c2 cell apoptosis by activating Nrf2/HO-1-mediated HIF1α/BNIP3 pathway. Artif Cells Nanomed Biotechnol 47:3657–3663
Zhang Q, Wang L, Wang S, Cheng H, Xu L, Pei G, Wang Y, Fu C, Jiang Y, He C, Wei Q (2022a) Signaling pathways and targeted therapy for myocardial infarction. Signal Transduct Target Ther 7:78
Zhang Y, Liu S, Ma J-L, Chen C, Huang P, Ji J-H, Wu D, Ren L-Q (2022b) Apocynum venetum leaf extract alleviated doxorubicin-induced cardiotoxicity through the AKT/Bcl-2 signaling pathway. Phytomedicine 94:153815
Zhou Q, Lin M, Feng X, Ma F, Zhu Y, Liu X, Qu C, Sui H, Sun B, Zhu A, Zhang H, Huang H, Gao Z, Zhao Y, Sun J, Bai Y, Jin J, Hong X, Zou C, Zhang Z (2020) Targeting CLK3 inhibits the progression of cholangiocarcinoma by reprogramming nucleotide metabolism. J Exp Med 217:e20191779